The Response of an Axisymmetric Model Tropical Cyclone to Local Variations of Sea Surface Temperature

SIMON W.-J. CHANG

JAYCOR, Alexandria, VA 22304

(Manuscript received 24 October 1978, in final form 5 February 1979)

ABSTRACT

An axisymmetric, multilayer, numerical tropical cyclone model with a well-resolved planetary boundary layer is used to test the response of local, instantaneous changes of sea surface temperature (SST). One experiment shows that the storm's intensity is steadily decreased as the SST in the inner 300 km is instantaneously cooled by 2°C. However, in the second experiment, in which the SST is cooled by 2°C outside the radius of 300 km, the storm shows no immediate and appreciable weakening. The intensity of the tropical cyclone in this case is maintained by enhanced evaporation in the inner 300 km and increased baroclinicity.

1. Introduction

In a recent paper by Anthes and Chang (1978), several numerical experiments were carried out to illustrate an axisymmetric model hurricane's response to an instantaneous, *uniform* change of sea surface temperature (SST). Their results show that the response of the tropical cyclone to an instantaneous, uniform change of SST is much milder than that was indicated by earlier numerical studies (e.g., Ooyama, 1969; Rosenthal, 1971; Sundqvist, 1972).

In reality, the SST and the storm-induced change of SST, however, are seldom uniform over the domain of a tropical cyclone. Observations indicate that the maximum storm-induced cooling in the ocean is concentrated over a small area near the center of the storm (e.g., Leipper, 1967; Black and Withee, 1976). Numerical simulations with ocean models have also demonstrated that most of the ocean's response to hurricane winds occurs near the center of the storm (e.g., O'Brien and Reid, 1967; Suginohara, 1973; Kuo and Ichiye, 1977; Chang and Anthes, 1978). It is therefore interesting to examine the response of the model hurricane to changes of ocean temperature at small radii.

We use the quasi-steady-state model hurricane in Anthes and Chang (1978) as the control (HC). In the first experiment (H4), the SST is instantaneously decreased by 2°C within the radius of 300 km. This situation is analogous to a stationary hurricane sitting over the open ocean, which has been cooled due to storm-induced mixing and upwelling near the storm center. In the second experiment, the SST is decreased by 2°C outside the radius of 300 km. This experiment tests the sensitivity of the model hurricane to the SST changes away from the region of strong convection. The decrease of SST at large radii creates a warm pocket in the ocean. Namias (1973) found that such an environment is very favorable for the growth of the tropical cyclone. We decrease the SST at large radii instead of increasing the SST at small radii to delineate from the effect of the evaporation another important effect of the horizontal nonhomogeneity in the SST—namely, baroclinicity.

2. Review of the hurricane model

The hurricane model used in this study is identical to the one described by Anthes and Chang (1978). The model atmosphere is divided into nine layers with higher resolution in the lower atmosphere. The boundaries of the model layers are defined at $\sigma = 0.0, 0.10, 0.30, 0.68, 0.92, 0.94, 0.96, 0.98, 0.995$ and 1.0. The parameterization of the planetary boundary layer (PBL) of Busch *et al.* (1976) is incorporated to give better estimates of various fluxes in the surface layer as well as in the atmospheric mixed layer. The parameterization of the cumulus convection follows Kuo (1974) and Anthes (1977).

As described in Anthes and Chang (1978), a steady-state hurricane with a central pressure of 981 mb and a maximum wind of 34 m s^{-1} develops. Because of the rather coarse horizontal resolution (60 km inside the 1000 km radius) of the model, this steady-state hurricane is larger and weaker than other earlier model hurricanes. In addition, the hurricane eye is not well-defined as indicated by Figs. 3–5 in Anthes and Chang.

The motion fields feature a shallow inflow layer, a shallow outflow layer beneath the tropopause,

0027-0644/79/060662-05$05.25

and a deep cyclonic circulation in the inner region. The thermodynamic structure of the steady-state hurricane is characterized by a moist, isothermal boundary layer, a moist warm core, a moist warm outflow canopy, and a dry, warm region above the boundary layer outside the inner convective region.

The height of the hurricane PBL is ~500 m, below which the potential temperature and the specific humidity are nearly invariant with height. The flow in the PBL features subgradient tangential velocity and nearly constant cross-isobaric flow angles. The sensible heating from the ocean is insignificant, as the hurricane PBL is almost thermally neutral. The evaporation is strong at a rate of about 1 cm day^{-1} averaged over the inner 300 Km.

In Anthes and Chang (1978), two experiments were conducted with this steady-state model hurricane to investigate its response to an instantaneous 1°C increase (H3) and decrease (H2) in SST over all radii. In contrast to the large response of other model hurricanes, the Anthes and Chang model hurricane reacted in a rather mild fashion. The model hurricane adjusted its PBL to the SST changes and showed an increased (H3) or a decreased (H2) hurricane ocean coupling. Steady modifications of hurricane intensity were not evident until 8 h after the SST change.

3. General structure and budgets

The prescribed changes of SST are accomplished at 96 h of the control experiment. The resulting minimum sea level pressures and the maximum surface winds as a function of time of H4 and H5 are shown, in Figs. 1 and 2, respectively. The response of the minimum surface pressure is slow until 100 h, when rapid filling occurs. As in Experiment H2 in Anthes and Chang (1978), the initial delay is related to the adjustment of the hurricane

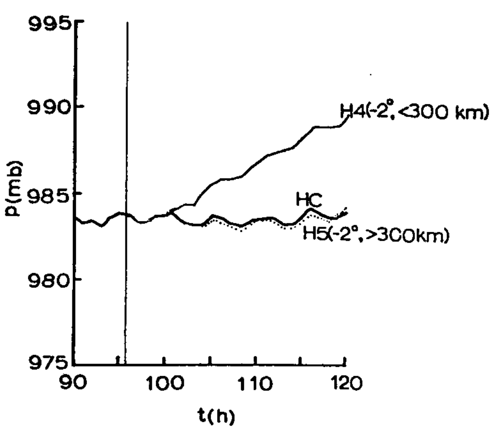

FIG. 1. The minimum sea-level pressure of experiments HC (control), H4 (−2°C, $r < 300$ km) and H5 (−2°C, $r > 300$ km).

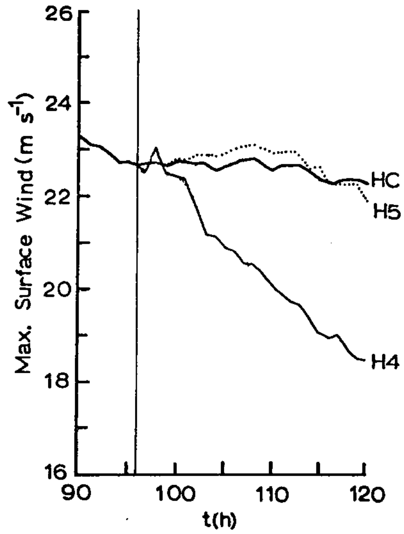

FIG. 2. The maximum surface wind speed of HC (control), H4 (−2°C, $r < 300$ km) and H5 (−2°C, $r > 300$ km).

boundary layer to the changed sea surface temperature, which leads to an initial reduction of kinetic energy (KE) dissipation. The maximum surface wind of H4 also exhibits an initial decrease followed by a recovery and finally a steady decrease. The amplitude of the oscillation of the maximum surface wind is larger than that of H2, probably because the adjustment of the boundary layer flow is more pronounced for the 2°C decrease of sea temperature. The final storm intensity at 120 h is weaker than H2.

The velocity fields of H4 at 120 h show a characteristic weakening hurricane circulation. The maximum inflow decreases to less than 10 m s^{-1}. The tangential circulation, which prevails in most of the hurricane atmosphere, is also weakened with maximum velocity of 25 m s^{-1} at the top of the hurricane PBL. The anticyclonic circulation at the outflow level, however, remains unchanged.

The model storm's behavior in H5, in which the sea temperature is decreased by 2°C beyond the 300 km radius, is quite different from that of H4. The minimum pressure and the maximum surface wind of H5 indicate that the storm is *intensified* slightly by the decrease of sea temperature at large radii, at least for nearly 20 h. At 120 h, the velocity fields of H5 are remarkably similar to those of HC. The radial and the tangential circulations of H5, however, are slightly stronger than those of HC between 100 to 115 h.

Fig. 3 illustrates the time series of five most important terms of the KE budgets inside the radius of 300 km for H4 and H5 [for budget calculation, see Anthes and Chang (1978)]. After the 2°C decrease of sea temperature at small radii, the KE conversion rate in H4 decreases from aobut 5×10^9

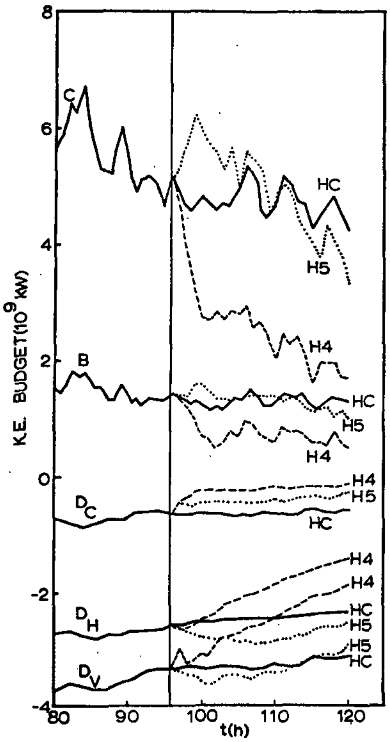

FIG. 3. Time series of the kinetic energy budget for the inner 300 km. C is the conversion from APE to KE; B, the net horizontal flux of KE across the lateral boundary at 300 km; $D_{C,H,V}$, the KE dissipation due to cumulus friction, horizontal diffusion and surface friction, respectively.

kW to 2.5×10^9 kW between 96 and 100 h. This rapid decrease is followed by a period during which the conversion rate gradually decreases to 2×10^9 kW. This temporal variation of the conversion rate is very similar to that of H2 except that in H4 the initial reduction is faster and the final level is lower. In contrast, the KE conversion rate in H5 is characterized by an initial increase to 6×10^9 kW. It remains higher than the conversion rate in HC until 110 h, then slowly decreases to about 4×10^9 kW.

The sudden increase of the KE conversion rate in H5 is presumably due to the increased baroclinicity introduced by the increase of the sea temperature outside of the radius of 300 km. As discussed by Anthes and Chang that the response time of the PBL is short, the instantaneous change of SST results in a temperature change in the hurricane PBL as the strong mixing tries to maintain a nearly adiabatic lapse rate. This temperature change in the hurricane PBL generates a stronger pressure gradient in the radial direction, which, in combination with the inflow in the hurricane PBL, produces an increase of the KE conversion.

Anthes and Johnson (1968) applied the concept of available potential energy (APE) to the hurricane. For a typical mature hurricane, they found that cooling in the outer region where the pressures are lower on isentropic surfaces contributes to the

TABLE 1. Enthalpy budget* (10^{15}W).

Simulation**	H_b	A	Q_c	Q_s
HC	3.000	−4.285	1.948	−0.006
H4	1.791	−1.985	1.093	−0.033
H5	3.292	−3.060	1.583	−0.007

* Only significant terms are shown.
** H_b horizontal flux of enthalpy across the lateral boundary at 300 Km radius.
A enthalpy change due to adiabatic vertical motion
Q_c enthalpy change due to cumulus convection
Q_s enthalpy change due to sensible heat exchange with the ocean.

generation of APE. In H5, the added APE is accompanied by an increase of KE conversion rate for the first 10 h following the cooling. Similarly, the initial rapid reduction of KE conversion rate in H4 is presumably a result of decreased baroclinicity introduced by the decrease of SST in the inner 300 km.

In spite of the initial intensification of the storm due to the increase baroclinicity in H5, the hurricane eventually weakens slightly compared with HC. This weakening is presumably caused by the reduction of evaporation over the outer region of the hurricane. The decrease of intensity, however, is far less than that in H4, and thereby indicates the greater importance of evaporation over the interior of the storm.

The enthalpy budgets within the radius of 300 km at 120 h for H4 and H5 are listed in Table 1. Note that the net horizontal influx of heat (H_b) across the lateral boundary at 300 km in H4 is only

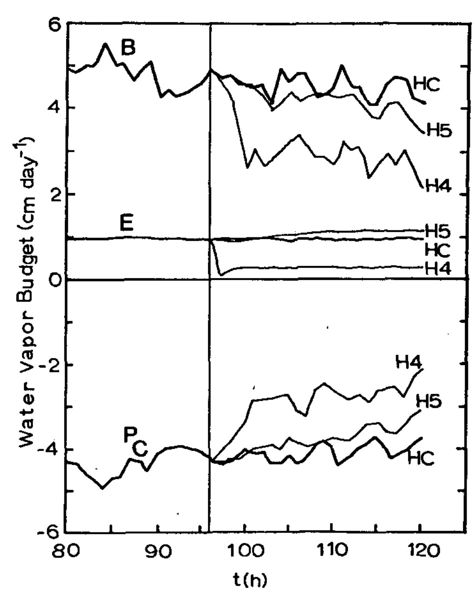

FIG. 4. Time series of the water vapor budget for the inner 300 km. B is the net water vapor flux across the lateral boundary; E, the surface evaporation; P_c, the precipitation rate from cumulus convection.

half of that in H5 despite the fact that the temperature in the hurricane boundary layer outside the radius of 300 km in H4 is higher than that in H5. This illustrates that the strength of the radial circulation in H5 is much stronger. Both the adiabatic cooling due to ascending motion (A) and the diabatic heating due to cumulus convection (Q_c) in H4 are smaller than their counterparts in H5. Compared with the control, the sensible heating from the ocean within the radius of 300 km is larger in H5. This occurs because the inflowing air is warmer than the sea surface in H4 whereas it is cooler than the sea surface in H5.

The moisture content in the hurricane PBL is different in H4 and H5 due to the different ocean temperature patterns. Time series of the important terms of the water vapor budget are shown in Fig. 4. Because the moisture content in the PBL is nearly saturated, or even supersaturated, with respect to the decreased ocean temperature within the radius of 300 km in H4, the evaporation rate immediately drops to nearly zero. Only after the PBL moisture within the 300 km radius is gradually depleted by the convection does the evaporation rate begin to recover. In contrast, the evaporation rate in H5 remains nearly unchanged for several hours, then increases to more than 1.1 cm day^{-1}. The reduced evaporation outside the radius of 300 km results in drier air being transported into the inner portion of the hurricane, where evaporation is then enhanced. The effect of drier inflow in H5 is also reflected by the gradual decrease of horizontal influx of moisture (B) after 105 h. Note that the decrease in B is not fully compensated for by the increase in evaporation in H5. Thus the precipitation decreases to only 3 cm day^{-1} and eventually the storm weakens.

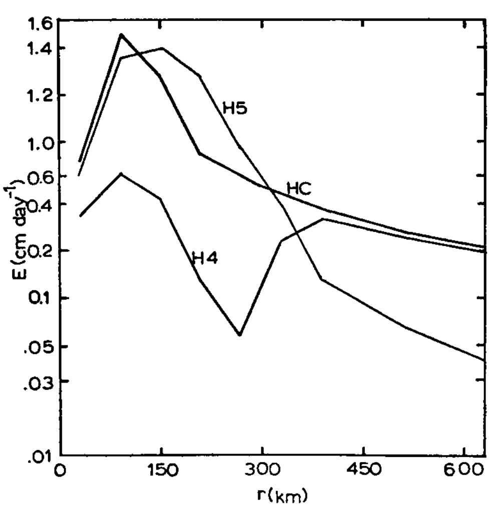

FIG. 5. The radial variation of surface evaporation for HC (control), H4 (-2°C, $r < 300$ km) and H5 (-2°C, $r > 300$ km).

4. The hurricane boundary-layer structure

Because of the cool ocean temperature of 120 h, the PBL heights of H4 in the inner region are lower than 300 m. The heights at large radii are also lower than the control. In H5, the PBL heights in the inner region remain relatively unchanged whereas they drop to below 200 m at large radii. The fact that the PBL heights at small radii in H4 are, in general, higher than the heights at large radii in H5, in spite of the same 2°C decrease in ocean temperature, indicates that the sea surface temperature is a more important factor in determining the PBL height at low wind speeds.

The process most sensitive to variations in sea surface temperature is the evaporation, because the variation of ocean temperature not only changes the surface stability but also the surface saturation specific humidity. Fig. 5 shows the radial variations of evaporation rate at 120 h for experiments HC, H4 and H5. The evaporation rate outside the radius of 330 km in H4 is only slightly lower than that of the control. This small reduction is associated with the weaker surface winds. The evaporation over the outer region sustains a moist inflow across the 300 km radius. When this moist air is transported over the 2°C cooler sea surface inside the radius of 300 km, the evaporation drops to an insignificant value because of the small difference between the surface specific humidity and the saturation specific humidity at the sea temperature. The evaporation increases with decreasing radius inside 270 km due largely to the strong surface winds and the drying effect of the cumulus convection. The maximum evaporation rate reaches 0.6 cm day^{-1} as compared with 1.5 cm day^{-1} of HC.

In H5, the evaporation outside the radius of 300 km is small. The relatively dry inflow causes a sharp increase of evaporation inside the radius of 300 km where the sea surface temperature is 2°C warmer. The evaporation rate exceeds that of the control experiment between radii of 150 and 300 km. Although the maximum evaporation rate of 1.4 cm day^{-1} in H5 is less than the maximum in HC, the area-averaged evaporation rate inside 300 km is higher.

The equivalent drag coefficients for momentum transfer at 120 h are listed in Table 2. Inside the radius of 300 km, the values of C_D in H4 are smaller than those in H5. Outside the radius of 300

TABLE 2. Equivalent drag coefficient C_D (10^{-3}).

Simulations	Radius (km) 60	120	180	240	300	360	420	480	540	600
HC	1.46	1.46	1.31	1.19	1.11	1.04	1.00	0.45	0.90	0.87
H4	1.29	1.32	1.21	1.04	0.96	0.99	0.93	0.93	0.90	0.82
H5	1.44	1.44	1.30	1.22	1.14	0.99	0.95	0.86	0.87	0.78

TABLE 3. Equivalent exchange coefficients C_E (10^{-3}).

Simulations	Radius (km) 30	90	150	210	270	330	390	450	510	570
HC	4.58	4.65	4.91	4.08	3.31	2.90	2.68	2.51	2.39	2.30
H4	3.26	3.00	2.16	0.76	0.40	1.72	2.46	2.31	2.20	2.10
H5	4.49	4.85	5.93	6.45	5.41	2.63	0.97	0.89	0.69	0.58

km, however, the values of C_D in H4 are larger than those in H5, an effect of the surface stability. The equivalent exchange coefficients for water vapor transfer, C_E, at 120 h are listed in Table 3. The values of C_E in H4 are generally larger than those in H5 outside 300 km, but they are smaller than those in H5 inside 300 km. The radial variation of C_E for these two experiments resembles the radial variation of the surface evaporation rate (Fig. 5). A discussion on the relative magnitudes of C_D and C_E can be found in Anthes and Chang (1978). Comparing the values of C_D and C_E of H4 and H5 with those of HC, one can demonstrate the stability-dependent nature in the interaction between the hurricane and the ocean.

5. Summary

Numerical experiments are carried out to test the tropical cyclone's response to local changes of SST. In the first experiment, after the SST is instaneously decreased by 2°C inside 300 km the model tropical cyclone shows a steady and rapid decrease of intensity. However, when the SST is decreased by the same amount at outside 300 km as in the second experiment, the model tropical cyclone shows only a very small decrease in intensity. The virtually constant intensity results from the cancelling of the positive effect due to the enhanced APE to KE conversion and the negative effect due to the decreased evaporation at large radii.

The results also suggest that the surface evaporation at small radii is more important than the surface evaporation at large radii for the development and maintenance of the tropical cyclone.

Results from these experiments indicate that for the case when a tropical disturbance centers itself over a pool of warm ocean water, as in Namias (1973), both the increased baroclinicity and increased supply of water vapor contribute to the rapid intensification of the storm.

Cautions should be taken in interpreting the magnitude of hurricane's response presented here, because a rather large and weak model hurricane has been used as the control. The results presented here, however, indicate that there exists a negative feedback between the ocean and the hurricane; namely, the increased stormed-induced cooling in the ocean caused by an intensifying hurricane will decelerate the intensification of the hurricane. This negative feedback mechanism has been investigated and discussed by Chang and Anthes (1979) using interacting hurricane and ocean models.

Acknowledgments. The author thanks Professor Richard A. Anthes for valuable discussions and suggestions. The reviewers' comments have greatly improved the clarity on several points in the manuscript. The research was supported by NOAA Grant 04-4-022-26 and Naval Environmental Prediction Research Facility Block Fund through NRL Contract N00173-78-C-421. Mrs. Margaret Steinert typed the manuscript.

REFERENCES

Anthes, R. A., 1977: A cumulus parameterization scheme utilizing a one-dimensional cloud model. *Mon. Wea. Rev.*, **105**, 270–286.

——, and S. W. Chang, 1978: Response of the hurricane boundary layer to changes of sea surface temperature in a numerical model. *J. Atmos. Sci.*, **35**, 1240–1255.

——, and D. R. Johnson, 1968: Generation of available potential energy in Hurricane Hilda (1964). *Mon. Wea. Rev.*, **96**, 291–302.

Black, P. G., and G. Withee, 1976: The effect of Hurricane Eloise on Gulf of Mexico. *Proc. Second Conf. Ocean-Atmosphere Interactions*, Seattle, Amer. Meteor. Soc., 123–155.

Busch, N. E., S. W. Chang and R. A. Anthes, 1976: A multilevel model of the planetary boundary layer suitable for use with mesoscale dynamic models. *J. Appl. Meteor.*, **15**, 909–919.

Chang, S. W., and R. A. Anthes, 1978: Numerical simulations of the ocean's nonlinear, baroclinic response to translating hurricanes. *J. Phys. Oceanogr.*, **8**, 468–480.

——, and ——, 1979: Mutual response of the tropical cyclone and the ocean. *J. Phys. Oceanogr.*, **9**, 128–135.

Kuo, H. L., 1974: Further studies of the parameterization of the influence of cumulus convection on large-scale flow. *J. Atmos. Sci.*, **31**, 1232–1240.

Kuo, H.-H., and T. Ichiye, 1977: A numerical study of the response of a barotropic ocean to a moving hurricane. *Tellus*, **29**, 561–571.

Leipper, O. F., 1967: Observed ocean condition and Hurricane Hilda, 1964. *J. Atmos. Sci.*, **24**, 182–196.

Namias, J., 1973: Birth of Hurricane Agnes-triggered by the transequatorial movement of a mesoscale system into a favorable large-scale environment. *Mon. Wea. Rev.*, **101**, 177–179.

O'Brien, J. J., and R. O. Reid, 1967: The nonlinear response of a two-layer baroclinic ocean to a stationary, axially-symmetric hurricane: Part I. Upwelling induced by momentum transfer. *J. Atmos. Sci.*, **24**, 197–207.

Ooyama, K., 1969: Numerical simulation of the life cycle of tropical cyclones. *J. Atmos. Sci.*, **26**, 3–40.

Rosenthal, S. L., 1971: The response of a tropical cyclone model to variations in boundary layer parameters, initial conditions, lateral boundary conditions, and domain size. *Mon. Wea. Rev.*, **99**, 767–777.

Suginohara, N., 1973: Response of a two-layer ocean to typhoon passage in the western boundary region. *J. Oceanogr. Soc. Japan*, **29**, 236–250.

Sundqvist, H., 1972: Mean tropical storm behavior in experiments related to modification attempts. *Tellus*, **24**, 6–12.